

## Hybrid Magnetic Bearing Regulation via Super Twisting Control

Mohamed S. Kandil<sup>1\*</sup>, Philippe Micheau<sup>2</sup>, João P. Trovão<sup>1</sup>, Loicq S. Bakay<sup>3</sup>, Maxime R. Dubois<sup>1</sup>

<sup>1</sup> e-TESC Laboratory, Department of Electrical & Computer Engineering, Université de Sherbrooke

<sup>2</sup> G.A.U.S, Mechanical Engineering Department, Université de Sherbrooke

Sherbrooke (Qc), Canada ({Mohamed.Kandil\*;Philippe.Micheau; Joao.Trovao; Maxime.Dubois }@USherbrooke.ca)

<sup>3</sup> Alstom Power

Sorel-Tracy (Qc), Canada (loicqbakay@gmail.com)

**Abstract**—A homopolar permanent magnet-biased magnetic bearing is a suitable solution to reduce power losses in active magnetic bearing systems. This configuration is complex due to the coupling between the coil-created magnetic fluxes and permanent magnet fluxes, besides being inherently a nonlinear, unstable, and multivariable system. One of the most recent topics in variable structure theory is represented by the higher order sliding modes (HOSM). In this paper, we propose the application of super twisting controller (STC) for the double loop robust stabilization of a rigid rotor horizontally supported by radial hybrid magnetic bearings. The efficiency of the applied controller is demonstrated via simulations in the presence of harmonic disturbances like vibration forces.

**Keywords**-, Magnetic Bearings, Super Twisting Control, Super Twisting Observer, Higher Order Sliding Mode

### 1. INTRODUCTION

In this paper we consider the radial PM-biased magnetic bearings (MB) proposed by Sortore *et al.* in [1], see Fig. 1. In this homopolar configuration, there is no variation of the flux polarity in the plane perpendicular to the axis of rotation. Subsequently, this design has less rotational losses besides having smaller coil and then less copper losses than heteropolar counterpart. A recent study [2] showed that this solution is more energy-efficient than pure active magnetic bearings. By employing homopolar hybrid magnetic bearing (HMB), the reliability will be increased as well by the extended lifetime of the power amplifier since the required amount of power is reduced. However, the HMB like all active MBs is a nonlinear, unstable, multivariable system on one hand. On the other hand, this approach is somewhat more complicated to construct and there is superposition and coupling of the coil –created magnetic flux and PM flux.

The problem addressed in this paper is to regulate the rotor movements at the operating speed despite the vibration forces due to rotor unbalance. To preserve the stability of the closed loop system as well as achieving a satisfactory performance in the presence of these periodical disturbances, the application of a robust control scheme is necessary. Decentralized PID control schemes have been used for regulating rigid rotors suspended with PM-biased MB systems due to the simplicity in

tuning their parameters [1][3][4]. However, the performance of these simple PID controllers could degrade at higher rotation speeds. Thus different unbalance and vibration compensation schemes have been developed to be implemented in conjunction with PID controllers [5]. The last draft of the American Petroleum Institute (API) standard for machinery with AMBs does not recommend using vibration compensation methods for new installations [6]. Therefore the transition from simple PID controllers to higher performance and more robust methods seems inevitable. Numerous advanced control methods have been proposed; such as modal PID control [7], gain scheduled control [8], feedback linearization [9], sliding mode control [10]–[13].

Sliding mode control (SMC) has been considered as an efficient robust control to provide satisfactory performance for nonlinear systems with uncertainties in system parameters and exogenous disturbances [14], [15]. On one hand, conventional sliding modes provide robust and high-fidelity performance in the presence of a class of bounded uncertainties, at least from a theoretical point of view [16]. On the other hand, the so called “chattering” phenomenon represents a serious implementation drawback. Chattering may occur due to the interaction between parasitic unmodeled dynamics and finite-frequency switching elements [16][14]. This high switching frequency phenomenon is dangerous and not acceptable in mechanical systems because it could lead to wear and tear in the actuator component. The most common approach to mitigate the chattering problem is to replace the discontinuous function in the conventional SMC with a smooth approximate function, this technique is known as “boundary layer” control. However, such an approximate function will affect the system performance while degrading robustness [15]. In

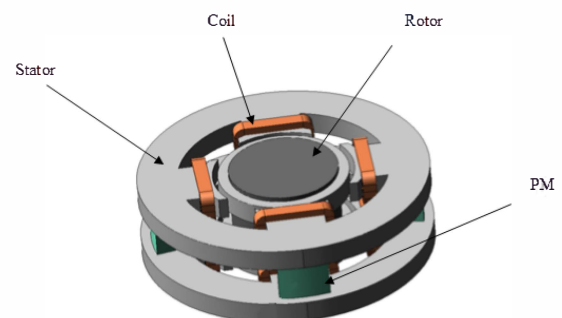


Fig. 1. Permanent magnet biased radial HMB

order to attenuate or eliminate the chattering problem and preserve the main advantages of the conventional SMC with respect to robustness, high performance, and simplicity, and finite time, super twisting control (STC) has been proposed [17]. Chattering effect is significantly reduced since STC is a continuous controller ensuring all the main properties of first order SMC [18]. However, the realization of STC for HMB requires the accurate calculation or measurement of successive time derivatives of the sliding variable. The development of robust exact differentiators (observers) based on the super twisting algorithm revealed the unique power of this approach [15][17]. This new generation of observers is known as super twisting observers (STO). Thus the development of a robust output-feedback controller is feasible through the combination of a STC with the STO. No detailed mathematical models of the plant is needed.

The goal is to employ the super twisting technique to design a robust controller to stabilize a rigid rotor supported on HMBs and to compensate the uncertainties and disturbances. If one wants to apply a continuous STC for relative degree two systems (i.e. differentiating the output twice so that the terms involving the control input appear), a STC based on a second order STO is needed in this case [18]. In this paper, a cascaded control structure is proposed. For the outer loop, a decentralized STO-STC is used for stabilization and unbalance compensation of a rigid rotor horizontally supported by a homopolar hybrid magnetic bearings (HMB). For the inner loop a STC is used such that the dynamics of the inner loop are faster than the outer loop and thus the rotor-bearing dynamics can be decoupled from the electrical dynamics. Modeling of the rotor-HMB system is presented first. The design method of the cascaded control is then presented. The efficiency of the proposed controller is confirmed via simulations in the presence of periodical disturbances like vibration forces.

## 2. MATHEMATICAL MODEL

Fig. 2 shows the basic structure of the rotor-bearing system. One terminal of the shaft is supported by a radial permanent magnet biased HMB while the other terminal is supported by a mechanical ball bearing. In a complete system, the rotor will be fully suspended using two HMB, but in the course of this paper, only one HMB is considered for simplification. The rotation is

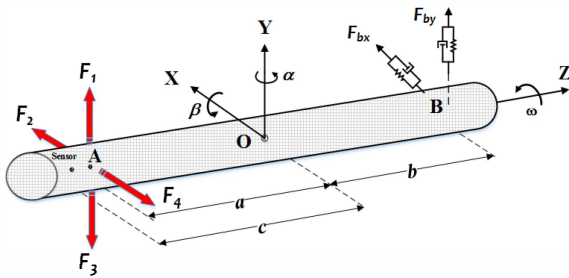


Fig. 2 Basic structure of the rotor-bearing system

realized through an induction electric motor which is connected to one end of the shaft with the means of a flexible coupling. The shaft displacements in both the horizontal and vertical directions are measured by two inductive position sensors.

### 2.1 Electromagnetic Force Formula

The radial HMB with two 4-tooth lamination stacks sandwiched with four axially arc-shaped magnetized permanent magnet (PM) segments is used [2]. Each tooth is wound with 100-turn coil and these stator coils are positioned along the vertical and horizontal axes to form the four electromagnetic (EM) poles. The 4 EM coils for each of the two axis are connected in series, thus the number of turns amounts to 400 turns per axis. Hence, the net flux in the air-gap is a combination of the bias and control fluxes. PMs provide the bias flux  $\phi_{pm}$  in the air-gap while EM coils generate flux  $\phi_c$  for stabilization and control. Fig. 3 illustrates these two main flux paths in the HMB. The vertical magnetic force  $F_{my}$  generated in the air-gap by the HMB is formulated as [19]

$$F_{my} = F_1 - F_3 = \left( \frac{\phi_1^2}{\mu_0 A_g} - \frac{\phi_3^2}{\mu_0 A_g} \right) \quad (1)$$

where  $\phi_1$  and  $\phi_3$  are the total fluxes in air gaps #1 and #3 respectively while  $A_g$  is the air gap area under one tooth. Since the electromagnetic force in (1) is nonlinear, Taylor expansion can be used for linearization around the operating point. The linearized bearing force  $f_b$  acting along the vertical direction at the geometrical center position can be written as:

$$F_{my} = -k_{sy} y_{bA} + k_{iy} i_y \quad (2)$$

where  $k_{sy}$ ,  $k_{iy}$  are the displacement and current stiffnesses of the vertical direction respectively and their calculation are given in [19] while  $i_y$  is the control current in the vertical direction. Likewise, the horizontal magnetic force of the HMB can be formulated as

$$F_{mx} = -k_{sx} x_{bA} + k_{ix} i_x \quad (3)$$

### 2.2 The Rotor-Bearing System Model

It is assumed that the rotor is symmetric and rigid, and the axial motion is decoupled from the radial ones. Therefore the radial dynamics can be represented by 4 degrees of freedom (DOF) while the axial dynamics is 1-DOF which is not being of particular interest here. The most straightforward approach to describe the rigid body dynamics is to use the displacements  $x_s$ ,  $y_s$  of its center of gravity and its inclinations  $\alpha$ ,  $\beta$  with respect to the inertial fixed reference [5]. Before the equations of motion are given, let us define their associated coordinate systems.

$\mathbf{q}$  : Center of Gravity (COG) coordinate

$\mathbf{q}_b$  : Bearings coordinate

$\mathbf{q}_{sc}$  : Sensors coordinate

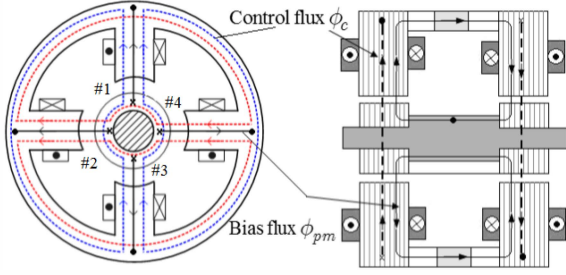


Fig. 3. The main flux paths of homopolar PM-biased magnetic bearing

Transformations for bearing and sensor coordinates can be done according to the following relations

$$\mathbf{q}_b = \mathbf{B}^T \cdot \mathbf{q} \quad \text{and} \quad \mathbf{q}_{se} = \mathbf{C} \cdot \mathbf{q}$$

where  $\mathbf{B}$  and  $\mathbf{C}$  are transformation matrices. The equation of motion for a rotor suspended with a HMB and a ball bearing can be written as

$$\mathbf{M}\ddot{\mathbf{q}} + \omega\mathbf{G}\dot{\mathbf{q}} = \mathbf{B}(\mathbf{F}_m + \mathbf{F}_b) + \mathbf{F}_{un} \quad (4)$$

$$\mathbf{y} = \mathbf{q}_{se} \quad (5)$$

where

$\mathbf{M}$  and  $\mathbf{G}$  are the mass and gyroscopic matrices respectively while  $\omega$  is the rotation speed. The electromagnetic force vector  $\mathbf{F}_m$  can be written as

$$\begin{aligned} \mathbf{F}_m &= \begin{bmatrix} F_{mx} & 0 & F_{my} & 0 \end{bmatrix}^T \\ &= -\mathbf{K}_s \mathbf{q}_b + \mathbf{K}_i \mathbf{i} \\ &= -\mathbf{K}_s \mathbf{B}^T \mathbf{q} + \mathbf{K}_i \mathbf{i} \end{aligned} \quad (6)$$

where

$$\mathbf{K}_s = \text{diag}[k_{sx}, 0, k_{sy}, 0],$$

$$\mathbf{K}_i = \text{diag}[k_{ix}, 0, k_{iy}, 0],$$

$$\mathbf{i} = [i_x, 0, i_y, 0]$$

The mechanical ball bearing force vector can be approximated as

$$\begin{aligned} \mathbf{F}_b &= \begin{bmatrix} 0 & F_{bx} & 0 & F_{by} \end{bmatrix} \\ &= -\mathbf{K}_{bb} \mathbf{B}^T \mathbf{q} - \mathbf{C}_{bb} \mathbf{B}^T \dot{\mathbf{q}} \end{aligned} \quad (7)$$

where  $\mathbf{K}_{bb}$  and  $\mathbf{C}_{bb}$  represents the stiffness and damping matrices for the ball bearing respectively.

Substituting for (6) and (7) in (4) and after manipulations gives

$$\begin{aligned} \mathbf{M}\ddot{\mathbf{q}} + (\omega\mathbf{G} + \mathbf{B}\mathbf{C}_{bb}\mathbf{B}^T)\dot{\mathbf{q}} + (\mathbf{B}\mathbf{K}_s\mathbf{B}^T + \mathbf{B}\mathbf{K}_{bb}\mathbf{B}^T)\mathbf{q} \\ = \mathbf{B}\mathbf{K}_i\mathbf{i} + \mathbf{F}_{un} \end{aligned} \quad (8)$$

The static unbalance forces acting on the system at the COG in  $x$  and  $y$  directions respectively can be modeled as

$$\mathbf{F}_{un} = \begin{bmatrix} 0 & m_e \varepsilon \omega^2 \cos(\omega t) & 0 & m_e \varepsilon \omega^2 \sin(\omega t) \end{bmatrix} \quad (9)$$

where  $m_e$  represents the unbalance mass while  $\varepsilon$  represents the offset of  $m_e$  from the COG. It is assumed that  $m_e \varepsilon = 0.01 \text{ kg.m}$ . These unbalance forces cause

vibrations in the rotating shaft and the amplitude of these vibrations is proportional to the square of rotational speed  $\omega$ . The objective is to regulate the rotor movements at the operating speed despite these unbalance forces while the displacements do not exceed 30% of the clearance of the safety bearings, i.e. 0.15 mm measured from the geometrical axis [6].

### 2.3 Electrical Dynamics

It is assumed that resistances and inductances of the coils are constants and equal to  $R$  and  $L$  respectively. The electrical dynamics in the system can be described by

$$\frac{d}{dt} \mathbf{i} = \frac{1}{L} \mathbf{V} - \frac{R}{L} \mathbf{i} \quad (10)$$

where  $\mathbf{V}$  is a vector of the input control voltages

$$\mathbf{V} = [v_{xA}, v_{xB}, v_{yA}, v_{yB}]$$

### 3. CONTROLLER DESIGN

STC is a well-known continuous second order SMC preserving all the main features of the first order SMC relative degree one systems with matched bounded uncertainties. Since the plant dynamics and the actuator dynamics represented by (8) and (10) respectively are block separated, i.e. the output of the actuator is the input to the plant, a cascaded control structure can be designed [14].

The following assumption are set to simplify the Rotor-bearing model in (8):

- The rotor-bearing system is symmetric and rigid.
- The system is at standstill.
- Sensors and bearings are collocated.
- Any coupling between the two bearings in  $x$ - $z$  plane and in  $y$ - $z$  plane are neglected.

Then the equations which describes a simplified 1-DOF hybrid magnetic suspension can be written as

$$\begin{aligned} \dot{x}_1 &= x_2 \\ \dot{x}_2 &= a_1 x_1 + b_1 u + f_1 \\ \dot{u} &= a_2 w - b_2 u \\ y &= x_1 \end{aligned} \quad (11)$$

where  $a_1 = \frac{-2k_s}{m}$ ,  $b_1 = \frac{2k_i}{m}$ ,  $a_2 = \frac{1}{L}$ , and

$b_2 = \frac{R}{L}$  The input control voltage is represented by  $w$

while the coil current is represented by  $u$ . The function

$f_1$  represents the matched uncertainties including the nonlinearities in system and the unbalance forces. It is assumed that the uncertainties are bounded, i.e.,  $|f_1| \leq \xi_1$  with bounded derivative  $|\dot{f}_1| \leq \xi_2$ .

The cascaded control structure is proposed in order to reduce the input-output relative degree of the simplified model described by (11). Fig. 4 shows the proposed

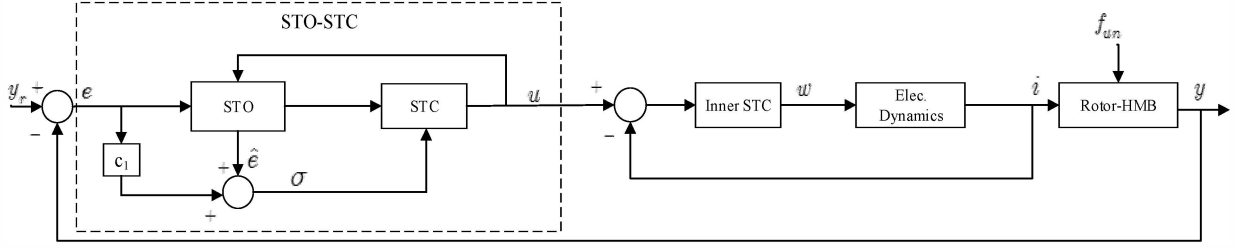


Fig. 4. Decentralized cascaded control structure

decentralized controller structure. The outer STC is designed in terms of control  $u$  which represents the reference current to the inner control loop. The inner STC is designed in terms of  $w$  in order to follow the reference current  $u$ .

### 3.1 Outer Loop Controller

A decentralized control structure is proposed to control each DOF of the radial HMB locally. The objective is to design two STO-STCs to regulate the rotor movement at the operating speed despite the vibration forces. In active magnetic bearings, regulating the rotor displacement around an equilibrium point, which is usually the geometrical center of the bearing, is an output-tracking problem. Thus it's necessary for the designed controller to be able to follow a fixed reference  $y_r$ . The output tracking error can be defined as

$$e = y_r - y \quad (12)$$

The controller  $u$  must be designed such that  $e \rightarrow 0$  in the presence of the uncertainties represented by the function  $f_1$ . The simplified 1-DOF magnetic suspension system represented by (11) is a relative degree two system with respect to the output variable  $y = x_1$ , therefore the application of the standard STC is not feasible here [18]. Thus we have to define the sliding variable of the form

$$\sigma = c_1 e + \dot{e} \quad (13)$$

where  $c_1$  is a real-valued constant chosen such that (13) has the desired behavior. Since we don't have exact information of  $\dot{e}$ , a robust exact differentiator (observer) is necessary to estimate its value [15]. The second order STO is given as [18]

$$\begin{aligned} \dot{\hat{e}}_1 &= \hat{e}_2 + k_1 |e_1 - \hat{e}_1|^{\frac{2}{3}} \text{sign}(e_1 - \hat{e}_1) \\ \dot{\hat{e}}_2 &= \hat{e}_3 + k_2 |e_1 - \hat{e}_1|^{\frac{1}{3}} \text{sign}(e_1 - \hat{e}_1) + u \\ \dot{\hat{e}}_3 &= k_3 \text{sign}(e_1 - \hat{e}_1) \end{aligned} \quad (14)$$

where  $e_1 = e$ ,  $e_2 = \dot{e}$ , and  $e_3 = \ddot{e}$ . Selecting the appropriate values of  $k_1$ ,  $k_2$ , and  $k_3$  guarantees that the

observer defined in (4) gives the robust exact estimation after a finite time [17]. Equation (13) can be rewritten as

$$\sigma = c_1 e_1 + \hat{e}_2 \quad (15)$$

The derivative of the sliding variable can be derived as

$$\begin{aligned} \dot{\sigma} &= c_1 \dot{e}_1 + \dot{\hat{e}}_2 \\ &= c_1 \hat{e}_2 - u + k_2 |e_1 - \hat{e}_1|^{\frac{1}{3}} \text{sign}(e_1 - \hat{e}_1) \\ &\quad + \int_0^t k_3 \text{sign}(e_1 - \hat{e}_1) d\tau \end{aligned} \quad (16)$$

The utilized STC can be defined as [18]

$$\begin{aligned} u &= c_1 \hat{e}_2 + k_2 |e_1 - \hat{e}_1|^{\frac{1}{3}} \text{sign}(e_1 - \hat{e}_1) \\ &\quad + \int_0^t k_3 \text{sign}(e_1 - \hat{e}_1) d\tau + \lambda_1 |\sigma|^{\frac{1}{2}} \text{sign}(\sigma) \\ &\quad + \int_0^t \lambda_2 \text{sign}(\sigma) d\tau \end{aligned} \quad (17)$$

Selecting the appropriate values of  $\lambda_1$  and  $\lambda_2$  of the controller in (17) guarantees the appearance of a 2-sliding mode  $\sigma = \dot{\sigma} = 0$  attracting the trajectories of the sliding variable (15) in finite time [17], [18]. For the existence condition proof of the proposed STO-STC, see [18].

*Remark:* the implementation of STC requires the measurement/ estimation of the first time derivative of the sliding variable. It is demonstrated in [18] that using a first-order exact differentiator/observer doesn't lead to a second order sliding motion because the derivative of the sliding variable contains a discontinuous component.

### 3.2 Inner Loop Controller

The goal is to design STC  $w$  such that the dynamics of the inner loop are faster than the outer loop and thus the rotor-bearing dynamics can be decoupled from the electrical dynamics. The STC can be designed as follows

$$w = c_2 |\hat{\sigma}|^{\frac{1}{2}} \text{sign}(\hat{\sigma}) + c_3 \int_0^t \text{sign}(\hat{\sigma}) d\tau \quad (18)$$

where  $\hat{\sigma} = i^* - i$  and  $i^* = u$  calculated according to (17).

Table I MODEL DATA FOR ROTOR-BEARING SYSTEM

Rotor mass (m)	61.9 kg
Rotor transverse moment of inertia ( $J_x = J_y$ )	4.79 kg m <sup>2</sup>
Rotor polar moment of inertia ( $J_z$ )	0.086 kg m <sup>2</sup>
Force to current factor ( $k_{ix} = k_{iy}$ )	609 N/A
HMB stiffness for horizontal motion ( $k_{xx}$ )	-28.05 N/mm
HMB stiffness for vertical motion ( $k_{yy}$ )	-47.8 N/mm
Nominal HMB air-gap length ( $G$ )	1 mm
Nominal safety bearing clearance length	0.5 mm
Bias current for vertical direction ( $I_{y0}$ )	0.5 A
Bias current for horizontal coils ( $I_{x0}$ )	0 A
Coil resistance (R)	1.137 $\Omega$
Coil inductance (L)	0.136 H
Dc voltage supply	100

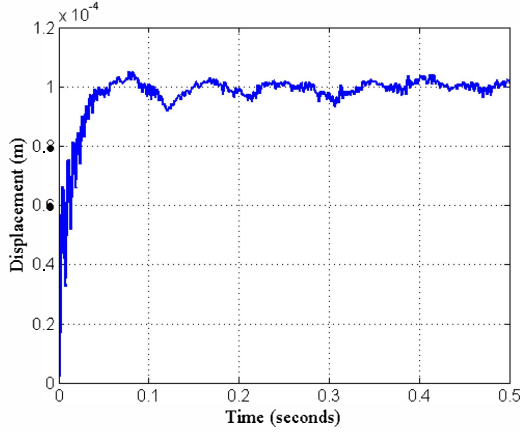


Fig. 5. Regulation performance of the closed loop system

#### 4. SIMULATION RESULTS

This section illustrates the performance of the controller through simulation results. The rotor-bearing system described in (8) is modeled in MATLAB Simulink environment. The sampling time for simulation is set to 0.1 ms. Table I indicates the model data used in this simulation. Table II indicates the design parameters of the cascaded control used in this work. White noise has been added to the displacement measurement signals. The noise magnitude is 1% of the measurement signal magnitude with the sampling time of 0.1 ms. To evaluate the tracking performance of the proposed controller, a step function of 0.1 mm is applied to set point of the horizontal direction. Fig. 5 shows that the controller achieves high precision tracking with no overshoot. Evolution of the estimation error of the second order STO is shown in Fig. 6. To evaluate the efficiency of the closed loop system to reject the vibration forces, the unbalance forces represented by (9) are incorporated into the simulation.

Fig. 7 shows the rotor orbits at bearing A for a rotation speed of 3000 RPM and demonstrates the efficiency of the STC to achieve the required objective. It is obvious that the obtained rotor orbit is much less than the

Table II DESIGN PARAMETERS FOR CASCADED CONTROLLER

		Horizontal Direction	Vertical Direction
STC Inner loop	$c_2$	20	20
	$c_3$	100	100
STC Outer loop	$c_1$	55	55
	$\lambda_1$	110	110
	$\lambda_2$	1	1
	$k_1$	70	70
	$k_2$	50	50
	$k_3$	120	120

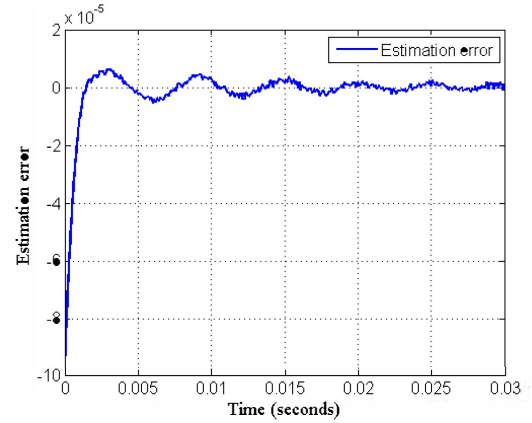


Fig. 6. Evolution of the estimation error w.r.t time

maximum allowable vibration level. Control efforts at the operating speed are presented in Fig. 8. As expected the control signal of the STO-STC is continuous and chattering free.

#### 5. CONCLUSION

Radial HMB is inherently unstable system besides being nonlinear, multivariable system. Due to the coupling between electromagnetic fluxes and permanent magnet fluxes, this special configuration of active magnetic bearings presents challenges in terms of their implementation and control. The suspended rotor experiences sinusoidal vibrating forces which increases with the rotation speed squared. The cascaded control structure is proposed in this work. The outer loop uses a decentralized second order observer based STC to robustly regulate the rotor movements at 3000 rpm in the presence of vibration forces due to rotor unbalances. The maximum vibration level is less than 30  $\mu$ m with a DC power supply limited to 100 V. A STC is used for the inner loop. The proposed STO achieves high convergence estimation in the presence of white noise. The robust high accuracy performance of the used controller is checked and confirmed by computer simulations.

#### REFERENCES

- [1] C. Sortore, P. Allaire, and E. Maslen, "Permanent magnet biased magnetic bearings, design,



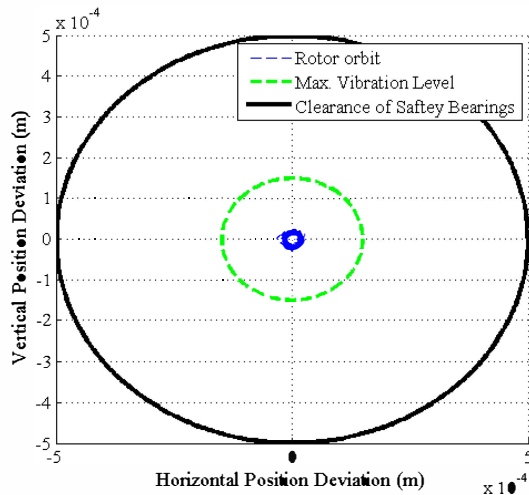


Fig. 7 Rotor orbit at bearing A

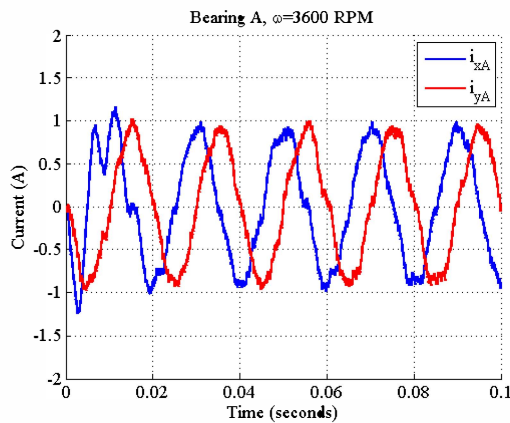


Fig. 8 Control currents at 3000 rpm rotation speed

construction and testing," *Second Int. Symp. Magn. Bear.*, 1990.

- [2] L. Bakay, M. Dubois, P. Viarouge, and J. Ruel, "Losses in hybrid and active magnetic bearings applied to Long Term Flywheel Energy Storage," *Power Electronics, Machines and Drives (PEMD 2010), 5th IET International Conference on*, pp. 1–6, 2010.
- [3] V. Wadhvani, "Feedback Control of a Permanent Magnet Biased, Homopolar Magnetic Bearing System," Texas A&M University, 2011.
- [4] Y. Fan, A. Lee, and F. Hsiao, "Design of a permanent/electromagnetic magnetic bearing-controlled rotor system," *J. Franklin Inst.*, vol. 334, no. 3, 1997.
- [5] H. Bleuler, M. Cole, P. Keogh, R. Larssonneur, E. Maslen, Y. Okada, G. Schweitzer, A. Traxler, and E. H. Maslen, *Magnetic Bearings: Theory, Design, and Application to Rotating Machinery*. Berlin, Heidelberg: Springer Berlin Heidelberg, 2009.
- [6] S. Y. Yoon, Z. Lin, and P. E. Allaire, *Control of Surge in Centrifugal Compressors by Active Magnetic Bearings*. London: Springer London, 2013.
- [7] T. Dever, G. Brown, K. Duffy, and R. Jansen, "Modeling and Development of Magnetic Bearing

Controller for High Speed Flywheel System," in *2nd International Energy Conversion Engineering Conference*, 2004, no. September.

- [8] L. Hawkins, B. Murphy, and J. Kajs, "Application of permanent magnet bias magnetic bearings to an energy storage flywheel," *Fifth Symp. Magn. Suspens. Technol.*, pp. 1–15, 1999.
- [9] W. Tong and F. Jiancheng, "A feedback linearization control for the nonlinear 5-DOF flywheel suspended by the permanent magnet biased hybrid magnetic bearings," *Acta Astronaut.*, vol. 79, pp. 131–139, Oct. 2012.
- [10] R. Smith and W. Weldon, "Nonlinear control of a rigid rotor magnetic bearing system: Modeling and simulation with full state feedback," *Magn. IEEE Trans.*, vol. 31, no. 2, 1995.
- [11] S.-Y. Chen, "Intelligent Sliding-Mode Control for Five-DOF Active Magnetic Bearing Magnetic Control System," National Central University, 2009.
- [12] A. Rundell, S. V. Drakunov, and R. A. DeCarlo, "A sliding mode observer and controller for stabilization of rotational motion of a vertical shaft magnetic bearing," *IEEE Trans. Control Syst. Technol.*, vol. 4, no. 5, pp. 598–608, 1996.
- [13] M. S. Kandil, M. R. Dubois, J. P. Trovão, and L. S. Bakay, "A Sliding Mode Control of a Hybrid Magnetic Bearing for Wayside Flywheel Energy Storage Systems," in "accepted for (VPPC)", 2015 IEEE. IEEE, 2015.
- [14] V. Utkin, J. Guldner, and J. Shi, *Sliding Mode Control in Electro-Mechanical Systems*, 2nd ed. CRC press, 2009.
- [15] Y. Shtessel, C. Edwards, L. Fridman, and A. Levant, *Sliding Mode Control and Observation*. New York, NY: Springer New York, 2014.
- [16] C. Edwards and S. Spurgeon, *Sliding Mode Control: Theory And Applications*. Taylor & Francis, 1998.
- [17] A. Levant, "Higher-order sliding modes, differentiation and output-feedback control," *Int. J. Control*, vol. 76, no. 9–10, pp. 924–941, 2003.
- [18] A. Chalanga, S. Kamal, L. Fridman, B. Bandyopadhyay, and J. A. Moreno, "How to implement Super-Twisting Controller based on sliding mode observer?," in *2014 13th International Workshop on Variable Structure Systems (VSS)*, 2014, pp. 1–6.
- [19] A. Lee, F. Hsiao, and D. Ko, "Analysis and testing of magnetic bearing with permanent magnets for bias," *JSME Int. journal. Ser. C, Dyn. ...*, 1994.